AIAA 79-1515R

Blade-to-Blade Flow Effects on Mean Flow in Transonic Compressors

A. K. Sehra*
General Motors Corporation, Indianapolis, Ind.
and
J. L. Kerrebrock†
Massachusetts Institute of Technology, Cambridge, Mass.

This paper describes a method of introducing nonaxisymmetric effects into the axisymmetric flowfield computation for a highly-loaded compressor. The approach is centered around modeling of three important nonaxisymmetric phenomena that control the mean momentum and energy transfer processes. Apparent stresses are introduced into the mean flow momentum equations by pitchwise averaging. The concept of apparent entropy resulting from the production of fluctuation energy is introduced. An expression for mean rothalpy variation along the streamline is derived by pitchwise averaging of the energy equation. Mean-flow equations suitable for the streamline-curvature computational scheme are developed which include these three effects. An assessment of the importance of these effects and experimental verifications of the computational approach have been achieved by use of time resolved experimental measurements of the flow in the MIT Blowdown Compressor. The revised streamline-curvature procedure has been used to predict the axisymmetric (peripheral mean) flow. The agreement of predicted and measured rotor outlet tangential velocity is excellent. The results show that three-dimensional inviscid effects do not modify significantly the mean flow, and that the direct effect of apparent stresses on the mean flow is also small. The major deviations of the actual flow from the inviscid flow are due to the variations of mean rothalpy and the production of apparent entropy, both effects which are introduced in turbomachine aerodynamics for the first time here.

Nomenclature

$F, F_{rv}, F_{\theta v}, F_{zv}$	= blade force, viscous body force components per unit mass in the r, θ, and z directions
H, h	= total enthalpy, static enthalpy
I	= rothalpy defined by $I \equiv h + w^2/2 - (r^2\Omega^2)/2$
ℓ	= direction of computation in the meridional plane
m	= meridional streamline direction
P_0, P_s, P_t	= reference static, and total pressures
q	= total absolute velocity defined by $q = (v_r^2 + v_\theta^2 + v_z^2)^{1/2}$
r, r_c	= radial, radius of curvature direction
S	= entropy
T_t, T_s	= total temperature, static temperature
t	= time
$v, v', \bar{v}$	= absolute velocity, fluctuation, time average
$w, w', \bar{w}$	= relative velocity, fluctuation, time average
z	= axial coordinate
β	= mean relative flow angle defined by $\tan\epsilon = \bar{w}_\theta / \bar{v}_m$
ϵ	= blade lean angle in $\ell - \theta$ plane defined by $\tan\epsilon = -r(\partial\theta/\partial\ell)$
γ	= angle between the direction of computation (ℓ) and the radial direction, ratio of specific heats
λ	= blade thickness blockage factor
ρ	= density
$\Sigma_r, \Sigma_\theta, \Sigma_z$	= apparent stress terms appearing in the radial, pitchwise, and axial momentum equations
ϕ	= angle between the meridional and axial directions
Ω	= angular velocity of the rotor

Subscripts

i	= inviscid component
m	= meridional component, mean value
n	= component perpendicular to m direction
p	= pertaining to pressure surface
r, θ, z	= radial, pitchwise, and axial components
s	= pertaining to suction surface
v	= viscous component

Presented as Paper 79-1515 at the AIAA 12th Fluid and Plasma Dynamics Conference, Williamsburg, Va., July 23-25, 1979; submitted Aug. 14, 1979; revision received Sept. 11, 1980.

*Development Engineer, Compressor Aerodynamics, Detroit Diesel Allison Division. Member AIAA.

†Richard C. Maclaurin Professor; Department Head, Aeronautics and Astronautics. Fellow AIAA.

Introduction

THE objective of the work being described here is to provide a logically consistent method for predicting the axisymmetric mean flow in turbomachinery using all available information about the blade-to-blade flow variations, which are regarded as a perturbation on this axisymmetric mean. This is a logical step beyond currently available design systems, such as that given in Ref. 1 which uses two-dimensional blade element data defined on axisymmetric stream surfaces, and derived from cascade data such as that of Ref. 2 or from prior experience with such a flow model. It is a step before the ultimate technique of fully three-dimensional viscous computation of flow in turbomachines, which is becoming feasible although actual implementation is some time off.

Three-dimensional inviscid approaches to the blade-to-blade flow are complementary to the present effort, providing estimates of the pressure distributions on the blading and of the effects of vorticity shed due to variation of circulation in the spanwise direction. However, as shown by Thompkins[3] even the complete three-dimensional inviscid solution does

not provide an adequate description of the axisymmetric mean flow because it fails to account for strong blade-to-blade flows induced by viscous effects, such as spanwise flows in the blade boundary layers and wakes, shock/boundary-layer interactions, and secondary flows due to end-wall layers. Multi-two-dimensional approaches such as that of Novak and Hearsey[4] suffer from this same deficiency.

As will become apparent, the approach to be adopted here is somewhat intuitive. It has been made possible by the availability of a fully time-resolved description of the actual flowfield of a highly-loaded transonic compressor rotor. This description is used as input to and for verification of the flow model.

Formally, the approach is to average the momentum equations and the energy equation in the tangential direction, retaining averages of terms quadratic in the blade-to-blade flow variations. This technique was introduced by Ruden,[5] and dealt with in considerable detail by Smith,[6] Horlock,[7] and Fujii.[8] Smith concluded on the basis of essentially an inviscid argument that the quadratic terms did not contribute significantly to the radial momentum equation in his pioneering paper on the radial equilibrium equation of turbomachinery. More recently, Hirsch[9] has included the quadratic averages in the momentum equations, using estimates of perturbation velocities taken from isolated airfoil wake data. He found the contributions to the axisymmetric mean flow to be small. We term these contributions, to the momentum balance, apparent stresses in analogy to the Reynolds' stresses of turbulent flow theory.

Our work adds three new elements to these prior efforts. One is the use of blade-to-blade flow data from a transonic compressor to estimate the flow perturbations, as noted previously. The others are improved treatments of the rothalpy and entropy.

To the authors' best knowledge, all current axisymmetric flow models assume that the rothalpy based on mean flow properties is conserved along axisymmetric mean stream surfaces. We show here that the rothalpy defined in this way actually changes markedly along mean stream surfaces as a result of two effects. One is spatial transport of energy by apparent stresses; the other is conversion of mean flow kinetic energy to energy of fluctuations. Together these have a large effect on the mean flowfield.

In the Crocco formulation of the momentum equations the pressure gradient is replaced by its equivalent in gradients of rothalpy and entropy, and therefore the cross-streamtube gradient of the entropy plays an important role in governing the flow. Axisymmetric theories have in the past used estimates of entropy change along streamtubes based on the dissipation produced by viscous stresses, mainly on the blades. We propose here the concept of an apparent entropy based on the idea that so far as the axisymmetric mean flow is concerned, energy invested in flow fluctuations of a scale equal to or less than the blade spacing is essentially lost to dissipation. Further, dissipative work done by apparent stresses is assumed to result in an increase in the apparent entropy.

Whereas the nonconstancy of the mean rothalpy is a logical consequence of its definition, the appropriateness of the apparent entropy can at present be judged only by the accuracy with which the overall model predicts the axisymmetric mean flow. As we shall see, this prediction is excellent for the one rotor so far investigated.

Theoretical Formulation

Mean Rothalpy and Apparent Entropy

The rothalpy is defined as

$$I \equiv h + (w^2/2) - (r^2\Omega^2/2)$$

Pitchwise averaging of this definition by the procedure outlined in Ref. 10 gives

$$I_{avg} = \bar{h} + \frac{\bar{w}^2}{2} - \frac{\overline{w'^2}}{2} - \frac{r^2\Omega^2}{2}$$

which indicates that conversion of mean-flow kinetic energy ($\bar{w}^2/2$) to the energy of fluctuations ($\overline{w'^2}/2$) does not change the value of the average rothalpy. In keeping with the physical postulate that the energy of fluctuations is unavailable to the mean flow, the mean rothalpy is defined as

$$\bar{I} \equiv \bar{h} + (\bar{w}^2/2) - (r^2\Omega^2/2) \tag{1}$$

and as we shall see this quantity is not conserved along mean stream surfaces.

As noted in the Introduction, we postulate a production of apparent entropy as results of the production of fluctuation energy and of dissipation by "apparent stresses." The apparent entropy production along the streamline is therefore taken to be

$$T\frac{D}{Dt}S_{app} = \frac{D(\overline{w'^2}/2)}{Dt} + \phi_{app} \tag{2}$$

where ϕ_{app} is the dissipation associated with apparent stresses. It contains terms such as $\overline{w_j'w_k'}(\partial\bar{w}_k/\partial x_j)$, which are normally known as "production" terms in turbulent flow. They represent loss to fluctuations due to the existence of shear in the flow. The first term on the right-hand side of Eq. (2) represents the production of fluctuation energy along the streamline.

Rothalpy Variation

To arrive at an expression for the rate of change of mean rothalpy along the mean streamline a pitchwise average of the energy equation is required. The procedure involves equating the mean rate of gain of internal and kinetic energy to the mean rate of work from the pressure forces, centrifugal force, and the apparent stresses. A detailed derivation of $D\bar{I}/Dt$ in terms of fluctuating quantities is given in Ref. 10. The result is,

$$\frac{D\bar{I}}{Dt} = -\Bigg[\underbrace{\left\{\bar{w}_r\left(\Sigma_r + \frac{\overline{w_\theta'^2}}{r}\right) + \bar{w}_\theta\Sigma_\theta + \bar{w}_z\Sigma_z\right\}}_{\text{I}} - \Phi_{app}$$

$$+ \underbrace{\frac{\bar{D}}{Dt}(\overline{w'^2}/2)}_{\text{II}}\Bigg] + \frac{1}{\rho}\Bigg\{\underbrace{-\frac{\overline{D'p'}}{Dt}}_{\text{III}} + \underbrace{\frac{\overline{p'w_r'}}{\rho}\frac{\partial\rho}{\partial r}}_{\text{IV}} + \underbrace{\frac{\overline{p'w_z'}}{\rho}\frac{\partial\rho}{\partial z}}_{\text{V}}\Bigg\}$$

$$+ \Bigg\{\underbrace{\frac{\overline{D'w'^2}/2}{Dt}}_{\text{VI}} + \underbrace{\overline{\frac{D'}{Dt}(\bar{w}w')}}_{\text{VII}}\Bigg\} + \underbrace{W_{vis}}_{\text{VIII}} \tag{3}$$

where D'/Dt is the derivative following the fluctuations. W_{vis} represents the work associated with viscous stresses, and is given by

$$W_{vis} = \Bigg[\overline{\frac{\partial}{\partial r}\{\tau_{rz}w_z + \tau_{r\theta}w_\theta\}} + \overline{\frac{\tau_{rz}w_z}{r}} + \overline{\frac{\tau_{r\theta}w_\theta}{r}}$$

$$+ \overline{\frac{\partial}{\partial z}(\tau_{zr}w_r + \tau_{z\theta}w_\theta)}\Bigg] \tag{4}$$

Φ_{app} represents the dissipation caused by apparent stresses and is given by

$$\Phi_{app} = -\Bigg\{\overline{w_r'^2}\frac{\partial\bar{w}_r}{\partial r} + \overline{w_z'^2}\frac{\partial\bar{w}_z}{\partial z} + \overline{w_r'w_\theta'}\frac{\partial\bar{w}_\theta}{\partial r}$$

$$+ \overline{w_r'w_z'}\left(\frac{\partial\bar{w}_z}{\partial r} + \frac{\partial\bar{w}_r}{\partial z}\right) + \overline{w_z'w_\theta'}\frac{\partial\bar{w}_\theta}{\partial z}\Bigg\} \tag{5}$$

Σ_r, Σ_θ and Σ_z are the force terms resulting from apparent stresses and are given by

$$\Sigma_r = \frac{\partial}{\partial r}(\overline{rw_r'^2}) + \frac{\partial}{\partial z}(\overline{w_r'w_z'}) - \frac{\overline{w_\theta'^2}}{r} \tag{6a}$$

$$\Sigma_\theta = \frac{\partial}{\partial r}(\overline{w_r'w_\theta'}) + \frac{\partial}{\partial z}(\overline{w_z'w_\theta'}) + \frac{2\overline{w_r'w_\theta'}}{r} \tag{6b}$$

$$\Sigma_z = \frac{\partial}{\partial r}(\overline{w_r'w_z'}) + \frac{\partial}{\partial z}(\overline{w_z'^2}) + \frac{\overline{w_r'w_z'}}{r} \tag{6c}$$

For the axisymmetric case $\bar{D}/Dt = \bar{w}_m \partial/\partial_m$, where m is the coordinate along the mean streamsurface, as shown in Fig. 1.

The energy transport processes responsible for the variation of mean rothalpy along the streamline may be understood by examining the several terms of Eq. (3) numbered I-VIII. Term I represents the work associated with normal and shearing apparent stresses acting at the mean velocities.

Term II represents the rate of change of the kinetic energy of fluctuations along the meridional streamline. It is seen that an increase in kinetic energy of fluctuations along the streamline will result in a decrease of mean rothalpy, and this is consistent with the physical concept that the energy of fluctuations is not recoverable by the mean flow.

Term III can be interpreted as work done by the velocity fluctuations in correlation with pressure fluctuations. In fact, it can be compared to acoustic energy transport. Terms IV and V are interpreted as the production of energy of fluctuating pressure due to the density gradient. Term VI can be written as

$$\frac{\overline{D'w'^2/2}}{Dt} = w_r' \frac{\overline{\partial w'^2/2}}{\partial r} + w_z' \frac{\overline{\partial w'^2/2}}{\partial z}$$

and the individual terms in the right-hand side of this equation can be expressed as

$$w_k' \frac{\overline{\partial w'^2/2}}{\partial x_k} = \frac{\overline{\partial (w_k' w'^2/2)}}{\partial x_k} - w'^2/2 \frac{\overline{\partial w_k'}}{\partial x_k}$$

Here the first term on the right-hand side is viewed as the spatial transport of the "kinetic energy of fluctuations" due to velocity fluctuations. The second term represents the production of fluctuation energy due to spatial variation of fluctuating velocity.

Term VIII, which represents the effect of molecular viscosity, is responsible for the spatial transport of kinetic energy due to viscous shear stresses. This spatial transport process is always accompanied by viscous dissipation resulting in loss of mean relative total pressure. The loss of relative total pressure occurs due to the conversion of kinetic and pressure energy to heat energy. On the other hand, the loss associated with fluctuations is due to the conversion of mean flow kinetic energy to the energy of fluctuations.

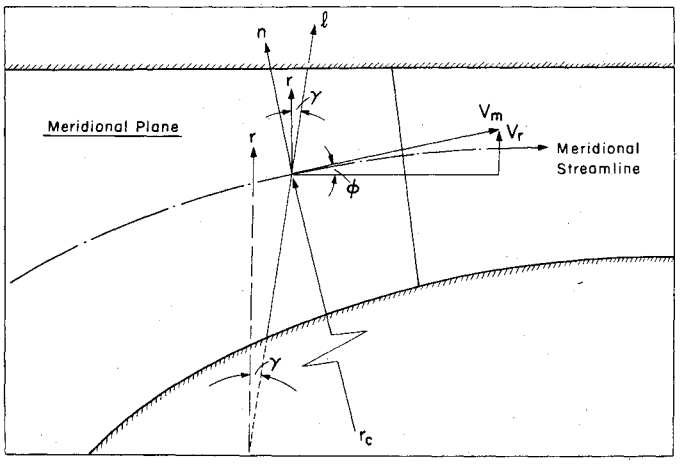

Fig. 1 Meridional cross section of compressor annulus, showing meridional m and computational ℓ coordinate directions.

Terms III-VIII cannot be estimated from the available experimental data, so must be neglected in the computations to follow. This neglect can be rationalized on the grounds that these terms are not as large as terms I and II. For example, term VIII, which represents work associated with viscous shear stresses, will be small, at least outside the blade row compared to the work done by apparent shear stresses. The spatial derivatives of fluctuating quantities are smaller than the spatial derivatives of apparent stresses so that terms III and VII can be neglected. Similarly, since the fluctuation in velocities is expected to be smaller than the mean velocity, $\overline{D'(w'^2/2)/Dt}$ will be small as compared to $\overline{D(w'^2/2)Dt}$.

With these deletions, Eq. (3) becomes

$$\frac{\partial \bar{I}}{\partial m} = -\left\{\sin\phi\left(\Sigma_r + \frac{\overline{w_\theta'^2}}{r}\right) + \tan\beta\Sigma_\theta + \cos\phi\Sigma_z\right\}$$
$$+ \frac{1}{\bar{v}_m}\left\{\overline{w_r'^2}\frac{\overline{\partial w_r}}{\partial r} + \overline{w_z'^2}\frac{\overline{\partial w_z}}{\partial z} + \overline{w_r'w_\phi'}\frac{\overline{\partial w_\theta}}{\partial r}\right.$$
$$\left. + \overline{w_r'w_z'}\left(\frac{\overline{\partial w_z}}{\partial r} + \frac{\overline{\partial w_r}}{\partial z}\right) + \overline{w_z'w_\theta'}\frac{\partial w_\theta}{\partial z}\right\}$$
$$- \frac{\partial}{\partial m}(\overline{w_r'^2}/2 + \overline{w_\theta'^2}/2 + \overline{w_z'^2}/2) \tag{7}$$

and this is the form proposed for inclusion in the flow model. All terms can be estimated from measurements of the blade-to-blade flow fluctuations which have been made for the MIT rotor.[3]

Entropy Production

Current practice for estimation of entropy increase through the rotor is to use experimental data from two-dimensional cascade tests. The cascade data of Ref. 2 is used widely. For transonic compressors, shock losses are superimposed on the viscous losses but it is well known that the entropy increase across a highly-loaded rotor near the hub and tip is larger than that estimated by this procedure.

The increased losses toward the casing have been attributed to the blade-passage shock by Miller et al.[11] The shock Mach number at the pressure surface is taken to be equal to the upstream relative Mach number, while the Mach number at the suction surface is estimated by a Prandtl-Meyer expansion on the blade suction surface. However, in the light of experimental studies carried out at the MIT Gas Turbine Laboratory, the foregoing procedure does not appear realistic for the rotor treated here. Density measurements made by Epstein[12] across the blade passage shock using a flow visualization technique indicated that the flow Mach number at the suction surface is not higher than that at the pressure surface. Thus the simple Prandtl-Meyer expansion is not applicable for the three-dimensional flow in this machine. It is, in fact, more realistic to assume that the mean relative Mach number at the blade inlet represents the uniform Mach number ahead of the blade passage shock. The entropy rise across the shock can then be estimated by the normal shock relation.

Viscous dissipation from kinetic energy to thermal energy results in an increase in entropy and a loss in the relative total pressure. It was argued in the Introduction that the presence of fluctuations at any point in the flow is equivalent to an unavailable form of energy as far as the mean flow is concerned, and that the existence of this unavailable energy (energy of fluctuations) creates an apparent increase in entropy, which influences the mean flow in the same manner as

the real entropy even before the process of conversion of fluctuation energy to thermal energy has actually taken place.

A relation between the production of apparent entropy and the production of fluctuation energy was established by the definition given in Eq. (2), which becomes

$$T\frac{\partial S_{app}}{\partial m} = -\frac{1}{v_m}\left\{\overline{w_r'^2}\frac{\partial \bar{w}_r}{\partial r} + \overline{w_z'^2}\frac{\partial \bar{w}_z}{\partial z} + \overline{w_r'w_\theta'}\frac{\partial \bar{w}_\theta}{\partial r} + \overline{w_r'w_z'}\left(\frac{\partial \bar{w}_z}{\partial r} + \frac{\partial \bar{w}_r}{\partial z}\right) + \overline{w_z'w_\theta'}\frac{\partial \bar{w}_\theta}{\partial z}\right\} + \frac{\partial \overline{(w'^2/2)}}{\partial m} \quad (8)$$

The total entropy increase through the rotor is taken as

$$(\Delta S)_{total} = (\Delta S)_{cascade} + (\Delta S)_{shock} + (\Delta S)_{app} \quad (9)$$

Mean Flow Equations for Streamline Curvature Computational Method

To test the preceding modifications of through-flow theory the streamline-curvature technique has been adopted. In its most general form the method employs a single equation of motion in the meridional plane along the direction of computation. For a nonbladed region the direction of computation normally is taken as the radial direction, but for computation at the inlet and outlet to a blade row, the direction of computation is made to coincide with the meridional projection of leading and trailing edges, respectively. Since most of the cascade data, such as flow angles and losses, are known at the blade trailing edge and depend on the conditions at the blade leading edge, this increases the accuracy of the computational scheme. This single equation of motion is transformed suitably by expressing radial and axial derivatives in terms of the derivatives in the meridional streamline direction and the direction of computation (m and ℓ directions in Fig. 1). The streamline curvature enters into the equation through the terms containing the radius of curvature and the slope of the meridional streamlines. The continuity equation is used along with this equation to fix the constant of integration. References 1 and 13 give detailed descriptions of the streamline-curvature technique. The mean-flow equations of Ref. 1 are rederived here so that the effect of blade-to-blade flow variations can be included.

Mean-Flow Equation of Motion in ℓ Direction

The method adopted for arriving at the mean-flow equation in the direction of computation is to first derive a mean-flow vector equation of Crocco's type and then take the scalar product of this equation with a unit vector in ℓ direction. The final equation is obtained by transforming the axial and the radial derivatives into the derivatives in the meridional and computational directions. Only an outline of the derivation is included here; the details are given in Ref. 10.

The mean-flow equation in Crocco's form can be written as

$$\underset{\text{I}}{\bar{w}\times(\nabla\times\bar{v})} = \underset{\text{II}}{\nabla\bar{I} - T\nabla\bar{S}} + \underset{\text{III}}{(\hat{r}\Sigma_{r\lambda} + \hat{\theta}\Sigma_{\theta\lambda} + \hat{z}\Sigma_{z\lambda})} \underset{\text{IV}}{-F_i} \underset{\text{V}}{-\overline{F_v}} \quad (10)$$

Here the apparent stress terms $\Sigma_{r\lambda}$, etc., include the effect of blade blockage. For example,

$$\Sigma_{r\lambda} = \frac{1}{\lambda}\left[\frac{\partial(\lambda\overline{w_r'^2})}{\partial r} + \frac{\partial(\lambda\overline{w_r'w_z'})}{\partial z} + \frac{\lambda(\overline{w_r'^2} - \overline{w_\theta'^2})}{r}\right]$$

In this equation, the effect of blade-to-blade flow variations enters directly through term III and indirectly through terms I and II. Term IV, which is the distributed blade force originating from the inviscid pressure field of the blade, also enters the equation through the pitchwise averaging process as a jump of pressure across the blade from the suction to the pressure surface. Term V represents the mean viscous force.

Taking the scalar product of Eq. (10) with a unit vector in the ℓ direction, and using the transformation relations

$$\frac{\partial}{\partial m} = \sin\phi\frac{\partial}{\partial r} + \cos\phi\frac{\partial}{\partial z}; \quad \frac{\partial}{\partial \ell} = \cos\gamma\frac{\partial}{\partial r} + \sin\gamma\frac{\partial}{\partial z}$$

Eq. (10) reduces to the following form:

$$\begin{aligned}\bar{v}_m\frac{\partial \bar{v}_m}{\partial \ell} &= \bar{v}_m\frac{\partial \bar{v}_m}{\partial m}\sin(\phi+\gamma) + \frac{\bar{v}_m^2}{r_c}\cos(\phi+\gamma) - \frac{\bar{w}_\theta}{r}\frac{\partial(r\bar{w}_\theta)}{\partial \ell} \\ &\quad - 2\bar{w}_\theta\Omega\cos\gamma + \frac{\partial \bar{I}}{\partial \ell} - T\frac{\partial \bar{S}}{\partial \ell} + \Sigma_{r\lambda}\cos\gamma + \Sigma_{z\lambda}\sin\gamma \\ &\quad - (F_{mi} + \overline{F_{mv}})\sin(\phi+\gamma) - (F_{ni} + \overline{F_{nv}})\cos(\phi+\gamma) \end{aligned} \quad (11)$$

This equation is further modified by eliminating $\partial \bar{v}_m/\partial m$ with the aid of the meridional-direction momentum equation and the continuity equation. The blade force terms $(F_{mi} + \bar{F}_{mv})$ and $(F_{ni} + \bar{F}_{nv})$ are expressed in terms of the rate of change of angular momentum and entropy production by using the procedure suggested by Wennerstrom.[14]

The final form of the analysis-type momentum equation in the ℓ direction, suitable for the computer program of Ref. 1 becomes

$$\begin{aligned}\frac{\partial \bar{v}_m^2}{\partial \ell}(1+\tan^2\beta) &= \frac{\bar{v}_m^2}{r_c}\frac{[1-\cos^2(\phi+\gamma)\bar{M}_m^2]}{\cos(\phi+\gamma)(1-\bar{M}_m^2)} \\ &\quad - \frac{\bar{v}_m^2\tan\beta}{r}\frac{\partial}{\partial \ell}(r\tan\beta) - 2\Omega\bar{v}_m\tan\beta\cos\gamma - \frac{\partial \bar{I}}{\partial \ell} - T\frac{\partial \bar{S}}{\partial \ell} \\ &\quad + \left\{\sin(\phi+\gamma)\left(\cos^2\beta + \frac{\gamma\bar{M}_m^2}{(1-\bar{M}_m^2)}\right) - \sin\beta\cos\beta\tan\epsilon\right\}T\frac{\partial \bar{S}}{\partial m} \\ &\quad - \frac{\bar{v}_m^2}{(1-\bar{M}_m^2)}\sin(\phi+\gamma)\left\{\frac{\sin\phi}{r}\left(1-\bar{M}_m^2\left(\tan\beta + \frac{r\Omega}{\bar{v}_m}\right)^2\right)\right. \\ &\quad \left. + \frac{1}{\lambda}\frac{\partial \lambda}{\partial \ell}\right\} + \frac{\bar{v}_m}{r}\frac{\partial}{\partial m}(r\bar{v}_\theta)\left\{\frac{\bar{M}_m^2}{(1-\bar{M}_m^2)}\sin(\phi+\gamma)\tan\beta - \tan\epsilon\right\} \\ &\quad - \frac{\bar{v}_m^2}{(1-\bar{M}_m^2)}\tan(\phi+\gamma)\frac{\partial \Phi}{\partial \ell} \\ &\quad + \left(\frac{\bar{M}_m^2}{(1-\bar{M}_m^2)}\sin(\phi+\gamma)\sin\phi + \cos\gamma\right) \\ &\quad \times \frac{1}{\lambda}\left(\frac{\partial}{\partial r}(\lambda\overline{w_r'^2}) + \frac{\partial}{\partial z}(\overline{w_r'w_z'}\lambda) + \frac{\lambda(\overline{w_r'^2} - \overline{w_\theta'^2})}{r}\right) \\ &\quad + \left(\frac{\bar{M}_m^2}{(1-\bar{M}_m^2)}\sin(\phi+\gamma)\cos\phi + \sin\gamma\right)\frac{1}{\lambda}\left(\frac{\partial}{\partial r}(\overline{w_z'w_r'}\lambda)\right. \\ &\quad \left. + \frac{\partial}{\partial z}(\overline{\lambda w_z'^2}) + \frac{\overline{\lambda w_r'w_z'}}{r}\right) + \left(\tan\beta\sin(\phi+\gamma)\frac{\bar{M}_m^2}{(1-\bar{M}_m^2)} - \tan\epsilon\right) \\ &\quad \times \frac{1}{\lambda}\left(\frac{\partial}{\partial r}(\overline{w_r'w_\theta'}\lambda) + \frac{\partial}{\partial z}(\overline{w_z'w_\theta'}\lambda) + \frac{2\lambda\overline{w_r'w_\theta'}}{r}\right) \end{aligned} \quad (12)$$

where

$$rv_\theta = r(v_m\tan\beta + r\Omega)$$

This equation has been used for computing the flowfield of the MIT blowdown compressor rotor. A few important

clarifications follow:

1) Equation (12) is applicable for the analysis problem within the blade row. For the unbladed region where the relative flow angles are not specified and where all blade related information such as blade forces, λ, ϵ are nonexistent, this equation is suitably modified to the format suitable for the design problem.

2) $r\bar{v}_\theta$ is found from the knowledge of β, blade velocity and the assumed value of $\bar{v}_m$.

3) Whereas the mean axial and radial velocities have been expressed in terms of the mean meridional velocity, the velocity correlations (apparent stresses) have been retained as the products of the axial and the radial velocity fluctuations. This is because the experimental data available for testing this formulation provided velocity fluctuations in the radial, axial, and the azimuthal directions most easily. The radial derivative of the apparent stresses has also been retained for the same reason. The axial derivative of the apparent stresses can, however, be transformed to the radial and the meridional derivatives by using the relation

$$\frac{\partial}{\partial m} = \sin\phi \frac{\partial}{\partial r} + \cos\phi \frac{\partial}{\partial z}$$

4) The mean rothalpy gradient $\partial \bar{I}/\partial \ell$ is estimated by integrating Eq. (7) in the streamwise direction.

5) The entropy gradients $\partial \bar{S}/\partial \ell$ and $\partial \bar{S}/\partial m$ are estimated from the entropy production model as formulated in Eq. (9).

6) The effect of radially directed apparent stresses is greatest because the effects of pitchwise and axial apparent stresses are scaled down due to their being nearly perpendicular to the ℓ direction.

Experimental Data from MIT Blowdown Compressor

For estimates of the apparent stress terms, and of $\partial \bar{I}/\partial \ell$ and $\partial \bar{S}/\partial \ell$ in Eq. (12), knowledge of velocity correlations and their derivatives is required. Experimental data from the MIT blowdown compressor rotor (as described in Ref. 15) was used for this purpose. Time resolved data on fluctuating pressures has been recorded by Thompkins[3] behind this highly loaded transonic rotor with the aid of a four-diaphragm probe. The data, which was digitized every 5 μs, provided the instantaneous values of the three components of absolute Mach numbers (M_r, M_θ, M_z) at different radial locations and two axial stations, 0.1 chord and 1.0 chord downstream of the rotor blade trailing edge. The instantaneous values of velocities were obtained by estimating static temperature with the aid of the Euler turbine equation written in the following form:

$$\frac{T_{t_2}}{T_{t_1}} = 1 + M_T(\gamma - 1)\left(\frac{r}{r_T}\right) M_{\theta_2}\left(1 + \frac{\gamma - 1}{2} M_2^2\right)^{-1/2} \left(\frac{T_{t_2}}{T_{t_1}}\right)^{1/2} \quad (13)$$

Here the subscripts 1, 2, and T refer to rotor inlet and outlet, and blade tip conditions.

The procedure adopted for estimation of the velocity correlations

$$\overline{v_r'^2},\ \overline{v_\theta'^2},\ \overline{v_z'^2},\ \overline{v_r'v_z'},\ \overline{v_r'v_\theta'},\ \text{and}\ \overline{v_z'v_\theta'}$$

involved three steps; namely, computation of the time averages, computation of the product of fluctuating quantities at each instant, and, finally, time averaging the products to obtain the velocity correlation terms.

Two points may be noted. First, the correlations of absolute velocity fluctuations are identical to those of the relative velocity fluctuations. Second, the time averaged flow with respect to the absolute frame of reference would be equivalent to the pitchwise averaged flow with respect to a frame of reference fixed to the blade if the flow were periodic with blade spacing. There is good reason to doubt that such periodicity exists. Figures 2-4 give the radial distributions of mean velocities and velocity correlations 0.1 and 1.0 chords downstream of the rotor trailing edge. These values were obtained by averaging the data over five blade passing periods, the maximum available in digital form. Averages were also taken over one, two, and three blade-passing periods and these were found to vary considerably towards the hub and the casing, thus indicating that the flow was not steady in the rotor coordinates. However, for this investigation, the averages over five blade-passing periods were taken as the best approximation to the true mean values. Reference 10 gives the details of averages over one, two, and three blade-passing periods.

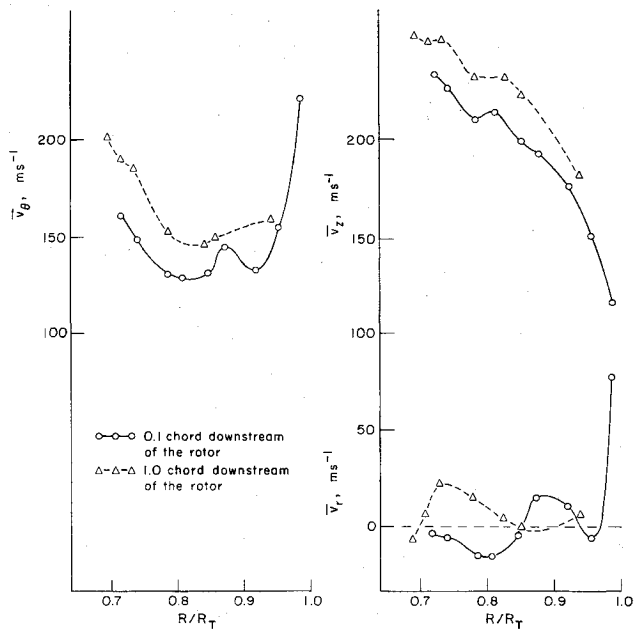

Fig. 2 Mean tangential, axial, and radial velocities as measured behind the MIT blowdown transonic compressor rotor at two axial stations.

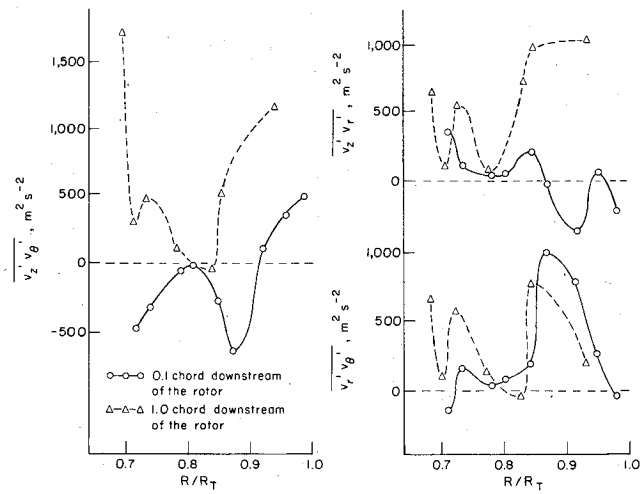

Fig. 3 Apparent shear stresses due to blade-to-blade fluctuations as measured behind the MIT blowdown transonic compressor rotor at two axial stations.

Mean Velocities

The mean velocities $\bar{v}_\theta$, $\bar{v}_z$, and $\bar{v}_r$ 0.1 and 1.0 chords downstream of the rotor are shown in Fig. 2. It is seen that the

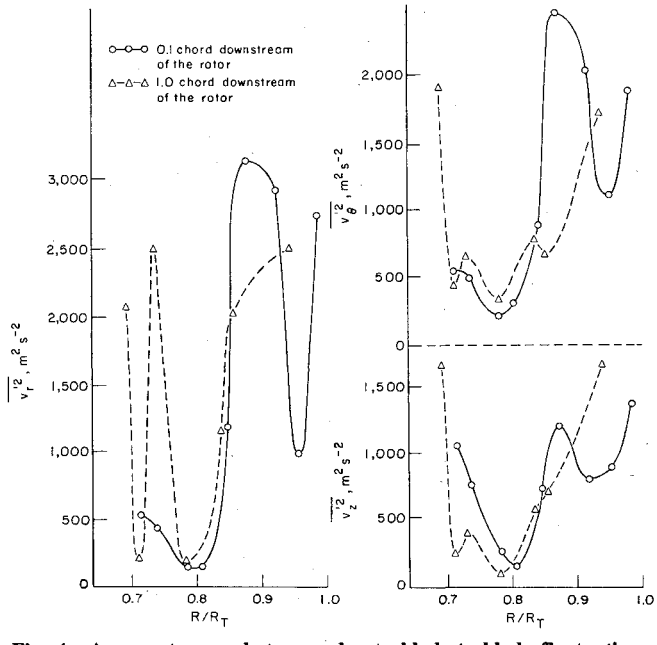

Fig. 4 Apparent normal stresses due to blade-to-blade fluctuations as measured behind the MIT blowdown transonic compressor rotor at two axial stations.

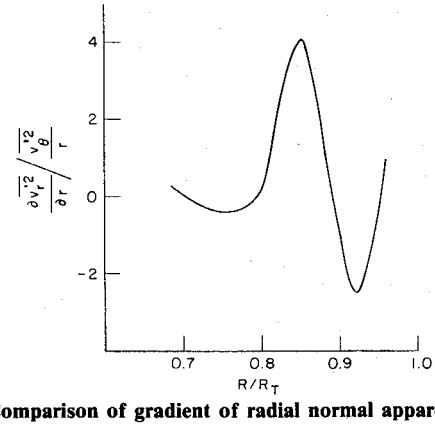

Fig. 5 Comparison of gradient of radial normal apparent stress to centrifugal force at outlet from rotor.

distributions of v_θ and v_z do not resemble the free vortex flow which was the intent of the original design. The mean radial velocity $\bar{v}_r$ shows an erratic behavior just behind the rotor and this is attributed to a possible flow separation near the hub. One chord downstream of the rotor, however, the erratic behavior of $\bar{v}_r$ has considerably diminished. The hump in the tangential velocity may be due to a shock/boundary-layer interaction in the vicinity of radius ratio 0.87.

It is also seen that there is a general upward shift in $\bar{v}_\theta$ and $\bar{v}_z$ between 0.1 chord downstream and 1.0 chord downstream of the rotor. The data at the two locations were derived from two separate tests, and this shift is tentatively attributed to a zero shift problem in the pressure transducers. Thus, only the shape of the curves at the two axial stations should be compared.

Velocity Correlations

It is seen from Fig. 3 that 0.1 chord downstream of the rotor, the apparent shear stresses $-\rho\overline{v_i'v_j'}$ would be of the order of 0.007 atm if the compressor had operated in ambient air and, hence, are fairly small compared to the pressure. On the other hand, there are rather steep gradients in the stresses, so their effect may be significant nevertheless.

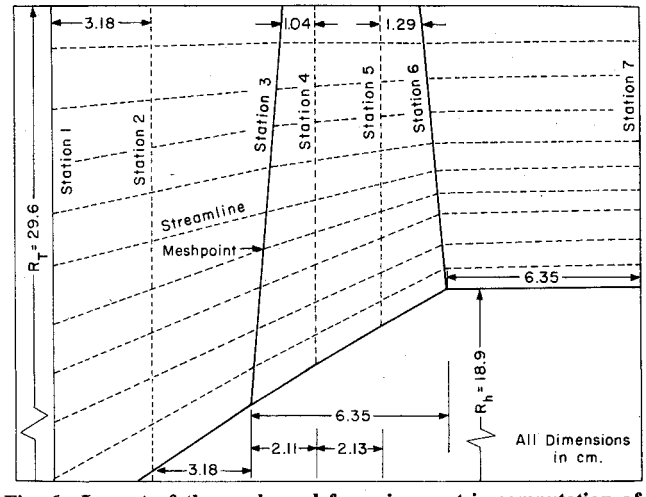

Fig. 6 Layout of the mesh used for axisymmetric computation of flow in the compressor annulus.

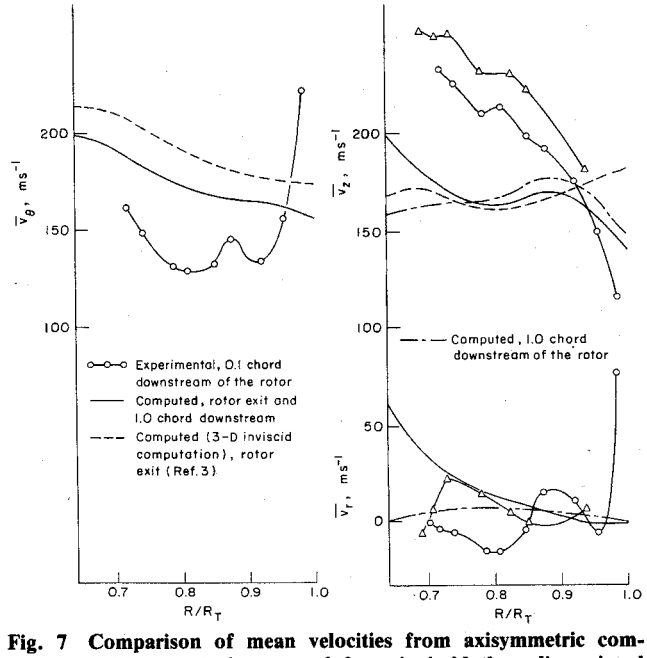

Fig. 7 Comparison of mean velocities from axisymmetric computation with cascade losses, and from inviscid three-dimensional computation, with experimental mean velocities.

The apparent normal stresses $-\rho\overline{v_i'^2}$, shown in Fig. 4, are much larger than the apparent shear stresses. It is observed that the gradients of $v_r'^2$ and $\overline{v_\theta'^2}$ are very large near $r/r_t = 0.87$ and near the casing. For example, the change of $\overline{v_r'^2}$ from nearly zero to 3000 m²/s² between $r/r_t = 0.8$ and 0.87 yields an effective pressure gradient of the order of 0.5 atm per unit radial distance, or in other terms half the static pressure per compressor radius. The magnitude of $\overline{v_r'^2}$ is indicative of the large radial flows in the wakes. An alternate way of assessing the order of magnitude of the term $\partial\overline{v_r'^2}/\partial r$ is to compare it with the centrifugal force $\bar{v}_\theta^2/r$ which approximately balances the radial pressure gradient. A plot of

$$\frac{\partial}{\partial r}\overline{v_r'^2} \Big/ \frac{\bar{v}_\theta^2}{r}$$

vs r/r_t is shown in Fig. 5. From this figure, it is seen that $\partial\overline{v_r'^2}/\partial r$, which is the most important apparent stress term in the ℓ-direction momentum equation, can become four times $\bar{v}_\theta^2/r$.

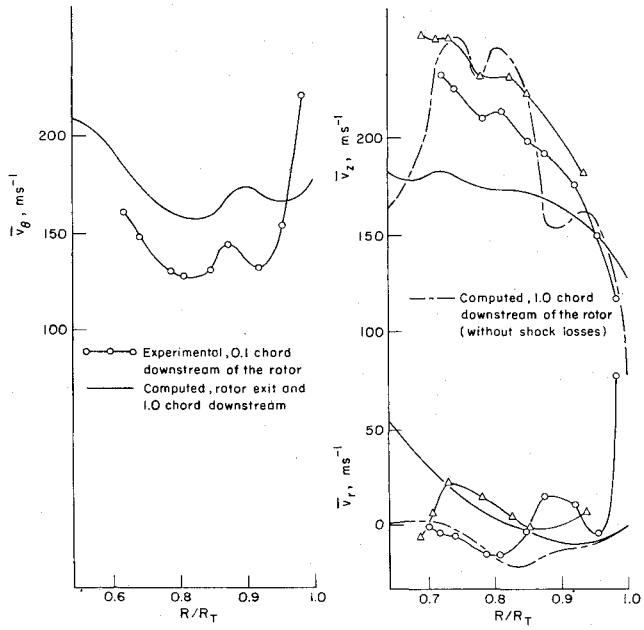

Fig. 8 Mean velocities computed with effects of apparent stresses, mean rothalpy variation, and apparent entropy variation, compared to experimental mean velocities. Note reproduction of peak in $\bar{v}_\theta$ at $R/R_T = 0.87$.

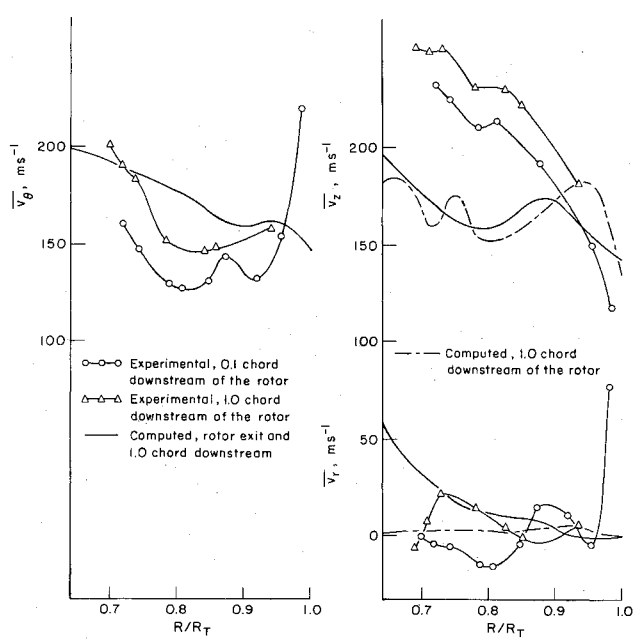

Fig. 9 Mean velocities computed with effects only of apparent stresses compared to experimental mean velocities.

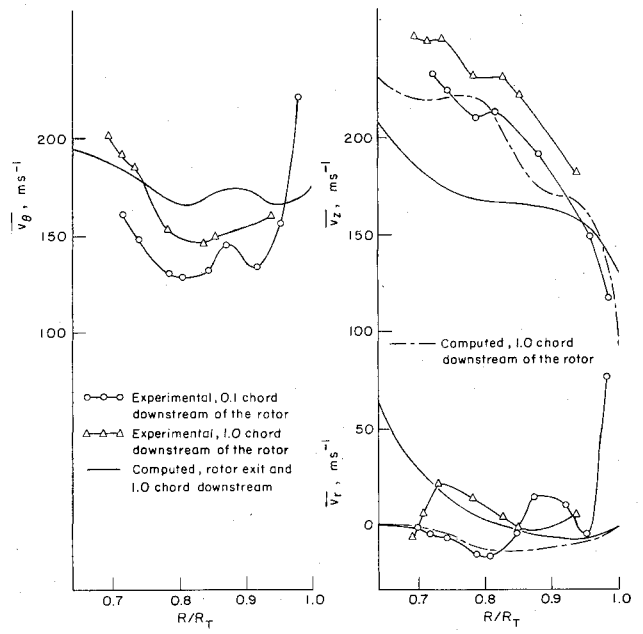

Fig. 10 Mean velocities computed with effect only of apparent entropy variation compared to experimental mean velocities.

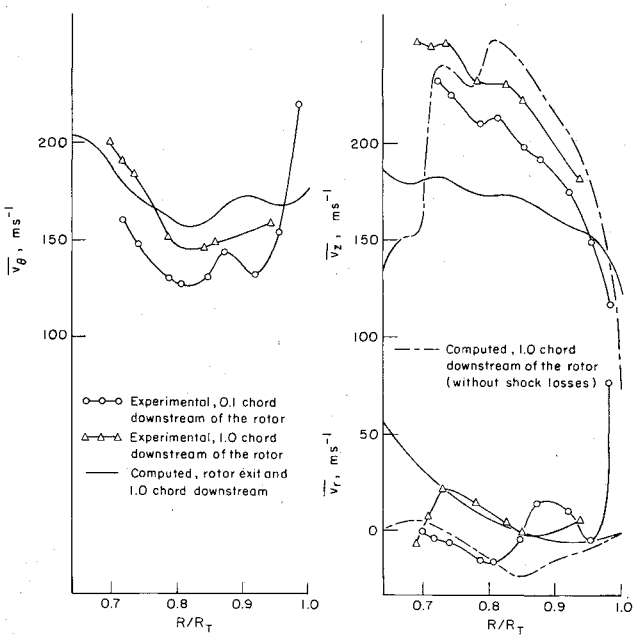

Fig. 11 Mean velocities computed with effect only of mean rothalpy variation compared to experimental mean velocities.

As can be seen from Figs. 3 and 4, the apparent stresses do not decrease very much 1.0 chord downstream, but there is a large change in the radial distribution of stresses.

Computed Mean Flow and Comparison with Experimental Results

The streamline-curvature program of Hearsey[1] was modified to include the nonaxisymmetric effects appearing in Eq. (12). The computational mesh used for this calculation is shown in Fig. 6. The input data for the analysis problem under investigation consisted of the blade exit relative flow angles β, geometrical features, mass flow rate, speed, compressor inlet conditions, losses (cascade and shock), and velocity correlation data. Some of the assumptions made for computing the mean flow are 1) the mean flowfield remains unchanged between the blade trailing edge and 0.1 chord downstream; 2) the derivatives of blade blockage $\partial\lambda/\partial x_i$ and density $\partial\rho/\partial x_i$ are small as compared to the derivatives of velocity correlations $\partial\overline{v_i'v_j'}/\partial x_i$; and 3) the velocity correlations are small at the blade leading edge and have a linear distribution along the meridional streamline within the blade row, to the measured value of the rotor outlet.

Numerical calculations were made to study the individual and combined effects of the three nonaxisymmetric phenomena. Figures 7-11 give the radial distribution of mean velocities $\bar{v}_\theta$, $\bar{v}_z$, and $\bar{v}_r$ at the rotor exit and one chord downstream. The results of numerical calculations shown in Figs. 8 and 11 for 1.0 chord downstream of the rotor do not include the shock losses since the calculation with shock losses did not converge at this station. The experimental values are also shown for the purpose of comparison.

Computed Flow with Cascade and Shock Losses

The distribution of mean velocities $\bar{v}_\theta$, $\bar{v}_z$, and $\bar{v}_r$ at the rotor exit (station 6) and at station 7, as computed with account for two-dimensional cascade losses, and shock losses are shown in Fig. 7. The predicted $\bar{v}_\theta$ has a negative slope from root to the tip and has completely failed to predict the local maximum and upturn at the tip found experimentally. The computed $\bar{v}_z$ does not show a steep fall near the casing, which is an important feature of the experimental $\bar{v}_z$. The $\bar{v}_r$ distribution that is mainly controlled by the large slope of the hub, decreases steeply from a large value at the hub to zero at the casing in conformity with the casing boundary conditions. A reversal of slope at two locations, as observed experimentally, has not been predicted by this computation.

Note, however, that the results of this computation show a close resemblance to the flowfield predicted by the three-dimensional inviscid computation of Ref. 3. This indicates that the three-dimensional inviscid effects per se do not alter the mean flowfield in a major way. The principal three-dimensional effects in this rotor are due to viscous interactions.

Effect of Nonaxisymmetric Phenomena on the Mean Flowfield

The computed flowfield with apparent stresses, mean rothalpy variations, and production of apparent entropy along the streamline is shown in Fig. 8. The combined effect of these nonaxisymmetric phenomena is found to change the free-vortex type velocity field to a distribution that resembles the experimental distribution. The agreement of rotor outlet tangential velocity $\bar{v}_\theta$ is excellent, reproducing an unusual peak that is not predicted by the usual computations. The observed difference in the absolute values of $\bar{v}_\theta$ at the rotor exit is attributed to a slight mismatch between the computed and experimental mass flows. Therefore, only the shape of the curves should be compared to assess the validity of the flow model. It is also seen that the predicted $\bar{v}_z$ at the rotor exit and mean velocity field at 1.0 chord downstream are in reasonable agreement with experiment. The disagreement between the predicted and the experimental distributions of $\bar{v}_r$ at the rotor exit may be due to a separation off the hub contour.

Influence of Individual Phenomena

The individual effects of apparent stresses, apparent entropy production, and mean rothalpy variation along the streamline are shown in Figs. 9-11. It is seen from these results that the direct effect of apparent stress terms on the mean flowfield is small, in spite of the fact, seen from Fig. 5, that the magnitude of the apparent stress terms is comparable to that of the centrifugal force $\bar{v}_\theta^2/r$. The largest contribution in reshaping the mean velocity field comes from the variation of mean rothalpy along the streamline. The effect of apparent entropy production, however, is considerably larger than that due to apparent stresses and, hence, it cannot be neglected.

Conclusions

The principal conclusions arising from this work are as follows.

1) The axisymmetric mean flowfield of a highly loaded transonic compressor rotor can be accurately predicted by a theory that includes the effects of blade-to-blade flows on the axisymmetric mean by peripheral averaging.

2) In highly loaded rotors the most important effects of the blade-to-blade flow on the axisymmetric mean arise from radial flows due to boundary layers and wakes.

3) Of the three effects modeled, namely, apparent stresses, mean rothalpy variation, and apparent entropy variation along stream surfaces, the last two dominate the departure of the real flow from the conventionally treated axisymmetric flow. Both effects have been treated here for the first time.

4) Although the results presented here are specific to the MIT blowdown transonic compressor, the computational procedure is applicable to any rotor for which estimates of the rotor-exit flow can be made, either theoretically or experimentally. It thus provides a systematic means for incorporating all knowledge of blade-to-blade flows in axisymmetric design computations.

Acknowledgment

This research was supported by the Air Force Aero Propulsion Laboratory, AFSC, under Contract F33615-76-C-2118, supervised by C. Herbert Law, Technical Contract Monitor.

References

[1] Hearsey, R. M., "A Revised Computer Program for Axial Compressor Design," Aerospace Research Laboratory, Wright-Patterson Air Force Base, Ohio, ARL-TR-7 5-0001, AD A009157, Vols. I and II, 1975.

[2] Johnson, B. and Bullock, R. O., editors, "Aerodynamic Design of Axial-Flow Compressors," NASA SP36, 1965.

[3] Thompkins, W. T. Jr., "An Experimental and Computational Study of the Flow in a Transonic Compressor Rotor," MIT Gas Turbine Laboratory Rept. 129, May 1976.

[4] Navak, R. A. and Hearsey, R. M., "A Nearly Three-Dimensional Interblade Computing System for Turbomachinery," ASME 76-FE-19 and 76-FE-20, Pts. I and II, 1976.

[5] Ruden, P., "Investigation of Single-Stage Axial Fans," NACA TM 1062, 1944.

[6] Smith, L. H. Jr., "The Radial-Equilibrium Equation of Turbomachinery," *Transactions ASME Journal of Engineering for Power,* Series A, Vol. 88, 1966, pp. 1-12.

[7] Horlock, J. H. and Marsh, H., "Flow Models for Turbomachines," *Journal of Mechanical Engineering Science*, Vol. 13, No. 5, 1971, p. 358.

[8] Fujii, S., "An Improved Method of the Local Loss Estimate in Axial-Flow Turbomachines," received Nov. 20, 1976, *ASME Journal of Fluids Engineering*.

[9] Hirsch, C., "Unsteady Contributions to Steady Radial Equilibrium Flow Equations," AGARD Conference on Unsteady Phenomena in Turbomachinery, CP-177, Paper 13, 1975.

[10] Sehra, A. K., "The Effect of Blade-to-Blade Flow Variations on the Mean Flowfield of a Transonic Rotor," Ph.D. Thesis, Aeronautics and Astronautics, Massachusetts Institute of Technology, Feb. 1979; also AFAPL-TR-79-2010.

[11] Miller, G. R., Lewis, G. W., and Hartmann, M. J., "Shock Losses in Transonic Compressor Blade Rows," *ASME Journal of Engineering for Power*, July 1961, pp. 235-241.

[12] Epstein, A. H., "Quantitative Density Visualization in a Transonic Compressor Rotor," M.I.T Gas Turbine Laboratory Rept. 124, Sept. 1975.

[13] Novak, R A., "Axisymmetric Computing Systems for Axial Flow Turbomachinery," Lecture 10, ASME Turbomachine Institute, Iowa State Univ., Aug. 1978.

[14] Wennerstrom, A. J., "On the Treatment of Body Forces in the Radial Equilibrium of Turbomachinery," Aerospace Research Laboratory, Wright-Patterson Air Force Base, Ohio, ARL-74-0150, 1974.

[15] Kerrebrock, J. L. et al., "The MIT Blowdown Compressor Facility," *ASME Journal of Engineering for Power*, Vol. 96, No. 4, 1974, pp. 394-405.